INTERNATIONAL ATOMIC ENERGY AGENCY
UNITED NATIONS EDUCATIONAL, SCIENTIFIC AND CULTURAL ORGANIZATION

INTERNATIONAL CENTRE FOR THEORETICAL PHYSICS
34100 TRIESTE (ITALY) - P.O.B. 586 - MIRAMARE - STRADA COSTIERA 11 - TELEPHONE: 2240-1
CABLE: CENTRATOM - TELEX 460392-1

SMR/406-25

THIRD AUTUMN WORKSHOP ON ATMOSPHERIC
RADIATION AND CLOUD PHYSICS
27 November - 15 December 1989

"Objective & Optimal Filtering Techniques with Applications to HIRS Cloud-Clearing"

C. SERIO
Dipartimento di Scienze Fisiche
Università di Napoli
Italy

Please note: These are preliminary notes intended for internal distribution only.

Objective and Optimal Filtering Techniques with Applications to HIRS Cloud-Clearing

C. SERIO
Dipartimento Scienze Fisiche, Universitá di Napoli, Italy

Introduction

Temperature sounding from polar orbiting satellite aimed at improving operational weather forecasting is currently performed by the TIROS Operational Vertical Sounder (TOVS) equipment. TOVS is an instrumental package consisting of two infrared radiometers, HIRS/2 (High resolution Infrared Radiation Sounder) and SSU (Stratospheric Sounding Unit), and MSU (Microvawe Sounding Unit).

HIRS and MSU units measure the upwelling radiation in the infrared and microvawe spectral regions respectively. Such radiances are affected, to a greater or lesser degree, by the presence of clouds. At infrared wavelengths the problem becomes acute since most clouds are almost opaque and as a consequence the measured radiances do not contain information on the thermodynamic state of the atmosphere below the cloud. On the other hand, in the microvawe region clouds usually have a neglegibile effect.

Most retrieval schemes produce atmospheric temperature profiles by operating on "clear-column" infrared radiances, that is radiances not affected by clouds, so a preliminary cloud-clearing step is required. This step consists of correcting the measured radiances to clear-column values, i.e. to the radiances which would be measured from the same temperature and humidity profiles in the absence of clouds.

In practice, such a task can be very complicated. If the measured radiances are only partly affected by clouds it is possible to use some empyrical relations between cloudy radiance, R_m, and clear radiance, R_c (e.g. the so called N^* method uses a linear relation between R_m and R_c), but in heavy cloudy conditions there not exhists any useful relation between the measured radiance and the one appropriate to clear conditions. Thus the measured data cannot be used to estimate clear-column radiances.

In such cases there are, in general, three possible alternatives:

a - to use only endogenous information, that is cloudy data are regarded as unmeasured or missing and estimates of clear-column values are provided from nearby clear measurements, if they exhist. From a mathematical point of view the problem consists of restoring a two-dimensional ridiance field from sparse data.

b - To use only exogenous information, e.g. MSU radiances which are generally less affected by clouds (Eyre and Watts 1987), suitable libraries of radiosonde profiles (Chedin and Scott 1984, Chedin et al. 1985).

c - To use both endogenous and exogenous information.

We shall consider approach c), anyway this lecture is mostly devoted to illustrate the mathematical aspects involved in point a).

From a mathematical point of view, point a) involves statiscal tools like linear smoothing or filtering. Linear filtering means convolution: a given function, $I(x,y)$ (the mesured values, in practice) is convolved with a suitable impulse response function, $U(x,y)$, to get the output, $O(x,y)$, that is the desired smoothed or restored field:

$$O(x,y) = \int_{-\infty}^{\infty}\int_{-\infty}^{\infty} I(\alpha,\beta)U(x-\alpha,y-\beta)d\alpha d\beta \tag{I}$$

In (I) there are two unknows, $O(x,y)$ and $U(x,y)$ and only one known ($I(x,y)$, i.e. the data). Thus to get solutions we have to determine the impulse response, $U(x,y)$, of the filter.

In general, if the determination of $U(x,y)$ is done "a priori", then one speaks of objective filtering. On the other hand if $U(x,y)$ is determined by means some suitable statistical principles, then one speaks of optimal filtering. As an example, if we use the Least Squares statistical principle, we say that the filtering is optimal in the Least Squares sense. The adjective "optimal" has no meaning by itself, if one does not make clear the statistical principle used.

The first part of this lecture deals with objective filtering, whereas the second one with optimal filtering in the Least Squares sense. Application examples to HIRS cloud-clearing will be performed in simulation using suitable clear radiance test fields.

Preliminaries

From now on, the scan pattern of a given HIRS/2 channel will be regarded as a two-dimensional (2-D) grid of spacing $(\Delta x, \Delta y)$; (see Fig. 1). Each node in the grid corresponds to a Field of View (FOV) in the original scan pattern.

According to the HIRS/2 scan pattern, the mean spacing between two adjacent FOVs is $\Delta x \approx 40$ km which is approximately equal to the line spacing (i.e. $\Delta y \approx 40$ km), thus we shall assume $\Delta x = \Delta y$. Furthermore the grid consists of $M = 56$ columns, since there are 56 FOVs for each scan line. On the other hand the number, N, of rows depends on the region or zone of interest.

Furthermore, in the following $V(i\Delta x, j\Delta y) \equiv V(i,j)$ will denote a generic variable or function defined on the grid, e.g. the measured radiance at the i-th scan line ($i = 1,\ldots,N$) and at the j-th FOV along the line ($j = 1,\ldots,M$; $\quad M = 56$).

A Gaussian objective analysis scheme to reconstruct clear-column HIRS radiance field from sparse data

Statment of the problem

As it was pointed out in the introduction, HIRS cloud-clearing problems present themselves as problems of reconstructing a radiance field from sparse data.

From a mathematical point of view we can state the problem as follows. Let $F(x, y)$ denotes a 2-D function and suppose we are given values of such a function at certain points (x_k, y_k); $k = 1, \ldots, N_p$, then we want to predict the values of F at some other points, say (x_j^*, y_j^*); $j = 1, \ldots, N_p^*$.

Such a problem has close relations with smoothing or filtering problems, thus we begin by analysing the filtering problem.

THE GAUSSIAN FILTERING SCHEME

Now we assume that the function F is known at each point. Anyway $F(x, y)$ is made up of $T(x, y)$, the "true" function, and $W(x, y)$, the noise, that is we have the additive signal and noise model:

$$F(x, y) = T(x, y) + W(x, y) \tag{1}$$

We wish to determine a spatial filter, with impulse response $U(x, y)$, in order to obtain an estimate $\hat{T}(x, y)$ of $T(x, y)$. In formulas we have:

$$\hat{T}(x, y) = \int_{-\infty}^{\infty} \int_{-\infty}^{\infty} F(\alpha, \beta) U(x - \alpha, y - \beta) d\alpha d\beta \tag{2}$$

In the Gaussian smoothing method the weighting function, $U(x, y)$, is taken to be a Gaussian density with zero mean and variance v^2:

$$U(x, y) = \frac{1}{2\pi v^2} \exp\left(-\frac{1}{2v^2}(x^2 + y^2)\right) \tag{3}$$

The only unknown in (3) is v^2. Its value determines the amount of smoothing and later it will be shown how to choice it properly.

For digital computing we have to discretize (2) and this can be done by direct approximation of the double integral in (2) by a double summation. However if we use a bit of mathematics it is possible to find a discrete approximation of (2) in which the only approximation is the grid spacing Δx.

By trasforming the filter equation in polar coordinates its expression becomes more useful for computational purposes. Assuming the current position (x, y) as origin, that is posing $(x, y) = (0, 0)$, we have:

$$\hat{T}(0, 0) = \int_0^{2\pi} \int_0^{\infty} F(r, \theta) \exp(-\frac{r^2}{2v^2}) r dr d\theta \tag{4}$$

where $r = (\alpha^2 + \beta^2)^{1/2}$. Because of its homogeneity features, the angular term in (4) can be integrated obtaining:

$$\hat{T}(0, 0) = \frac{1}{v^2} \int_0^{\infty} \tilde{F}(r) \exp(-\frac{r^2}{2v^2}) r dr \tag{5}$$

where

$$\tilde{F}(r) = \frac{1}{2\pi} \int_0^{2\pi} F(r, \theta) d\theta \tag{6}$$

thus $\tilde{F}(r)$ represents the average value of $F(r, \theta)$ on a circle of radius r.

Of course our function is sampled at discrete points, $(i\Delta x, j\Delta y)$, so that it is convenient to rewrite (5) scaling the lenghts to the spatial step, Δs ($\Delta s = \Delta x = \Delta y$) in the grid. With the variable substitution $\rho = r/\Delta s$, (5) becomes:

$$\hat{T}(0,0) = \frac{1}{\sigma^2}\int_0^\infty \tilde{F}(\rho)\exp(-\frac{\rho^2}{2\sigma^2})\rho d\rho \tag{7}$$

where $\sigma^2 = v^2/(\Delta s)^2$.

Now let us approximate the integral in (7) with a summation. Let us $a_0, a_1, \ldots, a_n, \ldots;\quad a_0 = 0$ an increasing sequence of real numbers, then (7) becomes:

$$\hat{T}(0,0) = \sum_{i=1}^{\infty}\frac{1}{\sigma^2}\int_{a_{i-1}}^{a_i} \tilde{F}(\rho)\exp(-\frac{\rho^2}{2\sigma^2})\rho d\rho \tag{8}$$

In practice the numbers $a_0, a_1, a_2, \ldots$, are simply the distances of the nearby points from the central FOVs, see Fig. 2.

Now if we approximate $\tilde{F}(\rho)$ in each integral appearing in (8) as the arithmetic mean between the values $\tilde{F}(a_{i-1})$ and $\tilde{F}(a_i)$, that is:

$$\tilde{F}(\rho) \approx \frac{\tilde{F}(a_{i-1}) + \tilde{F}(a_i)}{2}; \quad \text{with} \quad a_{i-1} \leq \rho \leq a_i \tag{9}$$

then (8) becomes:

$$\hat{T}(0,0) = \frac{1}{2}\sum_{i=1}^{\infty}(\tilde{F}(a_{i-1} + \tilde{F}(a_i)) \cdot I_i \tag{10}$$

with

$$I_i = \frac{1}{\sigma^2}\int_{a_{i-1}}^{a_i} \exp(-\frac{\rho^2}{2\sigma^2})\rho d\rho \tag{11}$$

Furthermore the quantity I_i can be written as:

$$I_i = \int_{a_{i-1}}^{a_i}(\cdot) = \int_0^{a_i}(\cdot) - \int_0^{a_{i-1}}(\cdot) = J_i - J_{i-1} \tag{12}$$

and (10), after a bit of algebra, can be re-written as:

$$\hat{T}(0,0) = \frac{1}{2}\Big(F(0,0)J_1 + \tilde{F}(a_1)J_2 + \sum_{i=2}^{\infty}\tilde{F}(a_i)(J_{i+1} - J_{i-1})\Big) \tag{13}$$

where

$$J_i = \frac{1}{\sigma^2}\int_0^{a_i} \exp(-\frac{\rho^2}{2\sigma^2})\rho d\rho; \quad i = 1, \ldots, n, \ldots \tag{14}$$

Finally, coming back to our discrete variables (i,j) we have the final result:

$$\hat{T}(i,j) = \frac{1}{2}\Big(F(i,j)J_1 + \tilde{F}(a_1)J_2 + \sum_{k=2}^{\infty}\tilde{F}(a_k)(J_{k+1} - J_{k-1})\Big) \tag{15}$$

In practice the values of $\tilde{F}(a_k)$ may be found by taking the average of points equally spaced on a circle of radius a_k:

$$\tilde{F}(a_k) = \frac{1}{N_p} \sum_{\substack{n,m \\ (n-i)^2+(m-j)^2=a_k^2}} F(n,m) \tag{16}$$

where N_p indicates the number of points in the summation and (i,j) denotes the position in the grid of the FOV we want to filter.

Of course to filter the entire field we have to move the centre of the smoothing window on each one of the nodes in the grid.

Now we shall consider how to determine the proper amount of Gaussian-filtering. As pointed out above the only parameter at our disposal is the standard deviation v of the linear operator (3), that is:

$$U(x,y) = \frac{1}{2\pi v^2} \exp\left(-\frac{1}{2v^2}(x^2+y^2)\right) \tag{17}$$

The transfer function of this linear operator is given by the Gaussian density function:

$$u(k_x,k_y) = \exp\left(-\frac{1}{2}v^2(k_x^2+k_y^2)\right) \tag{18}$$

where k_x, k_y denote wavenumbers along the x-axis and y-axis respectively. Now (18) also looks like a bell and its standard deviation is $1/v$, that is, the reciprocal of the standard deviation of the linear operator bell (17). Furthermore we note that each bell has its center on the origin of coordinates. Thus, we see that the transfer function (18) is a low-pass filter. For convenience, let use define the the cutoff radial frequency $k = (k_x^2 + k_y^2)^{1/2}$ to be the value $2/v$. Wavenumbers on the (k_x, k_y) plane outside the circle of radius k will be nearly completely attenuated upon passing through this filter. Thus a "small" value of v (i.e. a "large" value of $1/v$) must be prescribed if one wishes only a slight filtering. On the other hand a "large" value of v (i.e. a "small" value of $1/v$) must be prescribed if one wishes a strong filtering, that is a strong suppression of the noise.

However filtering always involves loss of resolution, thus a sort a compromise between loss of resolution and suppression of noise must be done.

For the HIRS cloud-clearing problem it turns out to be useful to design the Gaussian filtering scheme with a standard deviation v equal to $0.4 \cdot \Delta x$ or $\sigma = 0.4$. With such a choice only the adjacent FOVs of the current central FOV, (i,j) (see fig. 3) will be used to get an improved estimate of $T(i,j)$. Furthermore (15) becomes:

$$\hat{T}(i,j) = \frac{1}{2}\left(F(i,j)J_1 + \tilde{F}(a_1)J_2 + \tilde{F}(a_2)(J_3 - J_1)\right) \tag{19}$$

with $a_1 = 1, a_2 = \sqrt{2}$ and $J_1 = .95, \quad J_2 = J_3 = 1$.

It has to be noted that the summation of the weights in (19) is equal to one, that is the filtering scheme preserves the linear gradients of the field. Also it must be noted that the mean resolution of the final product is $\sqrt{2} \cdot \Delta x$ against Δx wich is the resolution of the original field.

Finally if the data $F(i,j)$ are affected by non-correlated noise, an expression of the error of $\hat{T}(i,j)$ can be found by means of the usual rule of variance propagation:

$$\hat{\sigma}^2(\hat{T}(i,j)) = \frac{1}{4}\left(\hat{\sigma}^2(F(i,j))J_1^2 + \hat{\sigma}^2(\tilde{F}(a_1))J_2^2 + \hat{\sigma}^2(\tilde{F}(a_2))(J_3 - J_1)^2\right) \tag{20}$$

where

$$\hat{\sigma}^2(\tilde{F}(a_k)) = \frac{1}{N_p^2} \sum_{\substack{n,m \\ (n-i)^2+(m-j)^2=a_k^2}} \hat{\sigma}^2(F(n,m)); \quad \text{with} \quad k = 1,2 \tag{21}$$

and with N_p ($N_P = 4$) being the number of points at distance a_k from the central node or FOV.

The Gaussian restoring scheme

In this section we come back to our original problem of reconstructing a clear radiance field from clear sparse data.

With reference to Fig. 3, let us suppose that the central FOV is cloudy and therefore we want an estimate, $\hat{T}(i,j)$, of the clear-column radiance at that position. Formally it suffices to put $F(i,j)$ in Eq. (19) equal to $\hat{T}(i,j)$, then solving for the unknown $\hat{T}(i,j)$ we have:

$$\hat{T}(i,j) = \frac{1}{1-\frac{1}{2}J_1} \cdot \frac{1}{2}(\tilde{F}(a_1)J_2 + \tilde{F}(a_2)(J_3 - J_1)) \tag{22}$$

Note that again the weights in (22) are normalised to 1 properly, thus the Gaussian restoring scheme also preserves linear gradients in the field.

However it may happen that some or all of the adjacent FOVs are themselves cloudy. For computational purposes it is convenient to define a flag, say $CCF(n,m)$, which assumes the value 1 if data at the node (n,m) is clear and the value 0 if data at the node (n,m) is cloudy. Inserting such a flag in Eq. (22) we can modify it in a form more useful for applications:

$$\begin{aligned}\hat{T}(i,j) = \frac{1}{1-\frac{1}{2}J_1} \cdot \frac{1}{2}\Big(J_2 \cdot \frac{1}{N_p} \sum_{\substack{n,m \\ (n-i)^2+(m-j)^2=1}} F(n,m)\cdot CCF(n,m) \\ + (J_3 - J_1)\cdot \frac{1}{N_p} \sum_{\substack{n,m \\ (n-i)^2+(m-j)^2=2}} F(n,m)\cdot CCF(n,m)\Big)\end{aligned} \tag{23}$$

Furthermore under the assumptions that the noise is a merely random process, we can use the variance propagation to get an estimate of the error $\hat{\sigma}^2(\hat{T}(i,j))$ of $T(i,j)$ by $\hat{T}(i,j)$:

$$\begin{aligned}\hat{\sigma}^2(\hat{T}(i,j)) = \big(\frac{1}{1-\frac{1}{2}J_1} \cdot \frac{1}{2}\big)^2 \big(J_2^2 \cdot \frac{1}{N_p^2} \sum_{\substack{n,m \\ (n-i)^2+(m-j)^2=1}} \hat{\sigma}^2(F(n,m))\cdot CCF(n,m) \\ + (J_3 - J_1)^2 \cdot \frac{1}{N_p^2} \sum_{\substack{n,m \\ (n-i)^2+(m-j)^2=2}} \hat{\sigma}^2(F(n,m))\cdot CCF(n,m)\Big)\end{aligned} \tag{24}$$

We want to note that the flags $CCF(n,m)$ are a normal product of preliminary cloud-clearing scheme used at present (Eyre and Watts 1987). Fig. 4 shows a pictorial representation of the matrix $CCF(i,j)$ as obtained by a preliminary cloud-clearing for overpass on 14 December 1987. In Fig. 4 FOVs or nodes with data detected as clear are indicated with a "·", whereas cloudy FOVs are indicated with a "*". There are 75 lines and the zone of interest is shown in Fig. 5. As you can see from Fig. 4 there was a heavy cloudy condition during the satellite pass. It is quite evident that clear data are not uniformly distributed within the field, since clouds tends to form clusters.

On the other side any restoring technique, including the Gaussian one, are very powerful if the data (clear data in our context) are randomly distributed within the area of interest. Thus, applying the above tool in real conditions, we need some suitable control index in order to know how far we are from the optimal situation.

Towards this objective we introduce the "average minimum distance", d_m, which gives, in the mean, the distance between a missing data (cloudy data) in the grid and its nearest clear data.

To determine such an index we need only the flag $CCF(n, m)$. Let us suppose $CCF(n_o, m_o) = 0$, that is the node (n_o, m_o) is cloudy, then we search for the nearest "clear" node, say (n_c, m_c), ($CCF(n_c, m_c) = 1$ and compute the distance, $d(k)$ ($\Delta x =$ one unit):

$$d(k) = ((n_o - n_c)^2 + (m_o - m_c)^2)^{1/2} \tag{25}$$

where $k = 1, \ldots, N_m$, with N_m being the number of unmeasured data. The average of these distances over the field is the average minimum distance, d_m:

$$d_m = \frac{1}{N_m} \sum_{k=1}^{N_m} d(k) \tag{26}$$

Together with d_m we also compute the "random average minimum distance", d_r. Let N_c be the number of measured data (clear data), with the help of a random number generator we distribute randomly and uniformly N_c "clear nodes or FOVs" across the grid; the result is a random flag $CCFR(n, m)$ that would have been observed if the original N_c clear FOVs were been uniformly distributed across the grid. Once $CCFR(n, m)$ is generated, we get d_r according to the above procedure for d_m.

As an example, in Tab. 1 we show both d_m and d_r for five different satellite passes above the area in Fig. 5. In Tab. 1 such passes are conventionally termed "1410", "1417", "1507", "1721", "1817". Their common characteristic is the high amount of cloudy FOVs, more than 80%. The flag CCF shown in Fig. 4 was obtained from the pass "1817". In such a case we have the highest value of d_m ($d_m = 6.3$ against $d_r = 1.69$), thus we are very far from the optimal condition (note that the distances shown in Tab. 1 are expressed in units of the grid spacing Δx, that is we have posed $\Delta x = 1$). It is interesting to note that d_r is very close to one unit also if the percentage of unmeasured data is equal to 90%.

However our Gaussian restoring scheme takes into account only the nodes which are inside or on the circle of radius $a_2 = \sqrt{2} \approx 1.41$. Thus the scheme will be successful in restoring the entire field only if $d_m \leq \sqrt{2}$. If $d_m \geq \sqrt{2}$, the technique will restore only a part of the field. In such a case with a suitable choice of the tuning parameter, v^2, of the filter we could design a scheme which takes into account FOVs up to a distance d_m from the central FOV. Then the scheme would be successful to restore the entire field.

However the value of d_m determines the mean spatial resolution of the final field. Thus, as an example, if d_m is equal to 6 the final resolution is not better than $6\Delta x$.

In such cases it is better to use exogenous information like MSU data which are less affected by clouds. In practice clear-column HIRS values can be estimated from MSU data using a regression relation (the relation is expressed in terms of brightness temperature; Eyre and Watts 1987). The horizontal resolution of MSU is less than resolution of the HIRS and it is about $4\Delta x$ where Δx is the HIRS grid spacing.

Using both Gaussian restoring scheme, with maximum radius equal to $\sqrt{2}$, and MSU data (regression relation) we can implement a two-step procedure in order to obtain estimates of clear-column HIRS radiances: the first step uses the Gaussian scheme developed above; if the scheme is not successful in restoring the entire field we use the regression relation among HIRS and MSU channels to fill the gaps left in the first step.

Unfortunately the HIRS-MSU regression relation gets biased results and the effect of such biases can be quite serious. Therefore, we have to remove them if possible.

At nodes where clear HIRS brightness temperature, $T_c(i,j)$, are obtained by the preliminary cloud-clearing scheme and by the Gaussian restoring scheme, we can also obtain values, $T_{MSU}(i,j)$, by the HIRS-MSU regression and hence to derive estimates, $B(i,j)$, of the bias between the two:

$$B(i,j) = T_c(i,j) - T_{MSU}(i,j) \tag{27}$$

Such sparse estimates of HIRS-MSU bias can be used in order to get values for the bias at all FOVs. After these values can be used to correct the brightness temperatures at FOVs where only the HIRS-MSU regression was used.

Towards this objective we have only to design a suitable Gaussian restoring scheme. We compute for the bias field the average minimum distance, d_m, and choice a value of the tuning parameter, v^2, in such a way that $a_{max} = d_m$, where a_{max} denotes the maximum radius in the Gaussian scheme.

The philosophy of the de-biasing procedure above is quite similar to the one used by Eyre and Watts, 1987, however the tools and algorithms are completely different.

Finally we have a complete scheme to reconstruct clear-column HIRS values from sparse data. The procedure is summarized in the flow-chart of Fig. 6.

NUMERICAL EXAMPLES

In this section we shall show some numerical examples of the technique above. The examples are obtained in simulation with the help of a test field. The test field consists of clear-column brightness temperatures in HIRS channel 5. Such values were computed by solving the forward problem of radiative transfer starting from a set of suitable radiosonde temperature profiles. The radiances so obtained were mapped on the HIRS scan pattern and converted to equivalent brightness temperatures. The number of data is 4200 and they are arranged in a grid with 75 rows and 56 columnns. The zone of interest is always the one shown in Fig. 5. Fig. 7 shows a mesh surface of the test field. The x-axis runs along the rows of the grid and the y-axis along the columns. According to the geometry of the HIRS scan pattern, the x-axis is approximately orientated along the direction North-South, whereas the y-axis along the direction Ovest-East.

There are a lot of interesting things to observe about the test field. There is a strong gradient along the North-South direction. Such a gradient explains more than 90% of the overall variance of the field which is about $5.2K^2$. On the other hand the variances along the lines are very small: less than $1K^2$ (see Fig. 8). This structure is typical of radiance fields at midlatitudes.

As a first example 80% of the data in the test field were randomly flagged as cloudy using a random number generator. The amount of "clear" data in the artificially generated cloudy field is 20% of the original number of data, but they are uniformly distributed across the area of interest. Thus an optimal situation is simulated but with a large amount of unmeasured (cloudy) data. To restore the field we do not need the MSU regression relation, since $d_m < \sqrt{2}$. The final product of the Gaussian restoring scheme is shown in Fig. 9. As it is possible to see the scheme is able to restore all of the main characteristics in the original field.

The following examples attempt to simulate real cloudy conditions. Now the data in the test field are flagged as clear or cloudy according to the flags, CCF, as obtained by a preliminary cloud-clearing for the overpasses indicated in Tab. 1. Tab. 2 summarizes the results. It is interesting to compare such results with the ones obtainable using only the MSU regression relation without de-biasing (Tab. 2).

The quantities shown in Tab. 2 were computed as follows. Let $T_t(i,j)$ denotes the brightness temperature in the test field and let $T_r(i,j)$ be the brightness temperature in the restored field, then at each node flagged as cloudy we compute the difference:

$$\Delta T(n,m) = T_r(n,m) - T_t(n,m) \quad (28)$$

In Tab. 2 "mean bias" is the average of the differences (28), while "rms error" is their standard deviation.

Figs. from 10 to 14 show histograms of the differences (Eq. 28) between restored field and test field (Gaussian scheme on the top; MSU regression relation without de-biasing on the bottom). As it is possible to note, the Gaussian scheme completely remove biases and also reduces the rms error.

Optimal Recursive Filters

Although the theory of 2-D recursive filters is, nowadays, well understood, their implementation is still a quite difficult task due to mathematical complexity. On the other hand 0-D recursive filters are very easy to implement and usually provide robust estimations. Here the term "robust" means: insensitive to small departures from the idealized assumptions for which the estimator is optmized.

As an example optimal (in the Least Squares sense) recursive filters are optmized to deal with Gaussian errors. If the filter is robust, then departures of the error distribution from the Gaussian distribution can be tolerated.

Thus in practice it turns out to be very useful to implement 2-D filtering scheme using 0-D filter equations. Later some examples will make clear what we mean.

The most general linear recursive filter takes a sequence $x(k)$ of input points (our data) and produces a sequence $\hat{s}(n)$ of outputs points (our desired estimates) by the formula:

$$\hat{s}(n) = \sum_{j=1}^{L_1} \beta_j \hat{s}(n-j) + \sum_{k=0}^{L_2} \alpha_k x(n-k) \tag{29}$$

Here the $L_2 + 1$ coefficients α_k and the L_1 coefficients β_j determine the impulse response of the filter.

If we want to design a low-pass filter it suffices to take $L_2 = 0$ and $L_1 = 1$:

$$\hat{s}(n) = \beta \hat{s}(n-1) + \alpha x(n) \tag{30}$$

Again we could determine a priori the two coefficients α and β, that is we could take again an "objective" approach.

However here we want to design an optimal filter. In the optimal approach it is not strictly required the two coefficients α and β to be constants. Thus we rewrite (30) as follows:

$$\hat{s}(n) = \beta(n)\hat{s}(n-1) + \alpha(n)x(n) \tag{31}$$

Now let $s(n)$ indicate the "true" signal, then our problem is to determine the coefficients $\alpha(n)$ and $\beta(n)$ in such a way that the mean square (m.s.) error $e(n)$:

$$e(n) = E\{(s(n) - \hat{s}(n))^2\} \tag{32}$$

is a minimum. In (32) $E\{\cdot\}$ denotes expectation.

To solve such a problem we have to make some assumptions about the structure of both "data" (i.e. the input sequence $x(n)$) and signal, that is the sequence $s(n)$. As usual we assume the additive noise and signal model:

$$x(n) = s(n) + w(n) \tag{33}$$

Furthermore we assume that the signal sequence $s(n)$ is wide-sense Markov:

$$E\{s(n) \mid s(n-1), s(n-2), \ldots, s(1)\} = E\{s(n) \mid s(n-1)\} \tag{34}$$

an the noise consists of orthogonal random variables with variance, $\sigma_w^2(n)$ that are also orthogonal to $s(n)$:

$$\begin{aligned} E\{w(i)w(j)\} &= 0; \quad i \neq j \\ E\{s(i)w(j)\} &= 0; \quad \forall i,j \end{aligned} \tag{35}$$

The appropriate normal equations which permit to get a solution for $\alpha(n)$ and $\beta(n)$ are (Papoulis 1965):

$$E\{(s(n) - \hat{s}(n))x(n)\} = 0 \tag{36}$$

and

$$E\{(s(n) - \hat{s}(n))x(i)\} = 0; \quad i = 1, 2, \ldots, n-1 \tag{37}$$

which give the solution:

$$\begin{aligned} \beta(n) &= \frac{e(n)}{\sigma_w^2(n)} \\ \alpha(n) &= \rho_1(1 - \beta(n)) \\ e(n) &= \frac{\sigma_s^2(1-\rho_1^2) + \rho_1^2 e(n-1)}{\sigma_s^2(1-\rho_1^2) + \rho_1^2 e(n-1) + \sigma_w^2(n)} \sigma_w^2(n) \end{aligned} \tag{38}$$

where σ_s^2 and ρ_1 are respectively the variance and the first serial correlation coefficient of the signal sequence. The iterative structure of the filter equations is quite evident. Also remember that $e(n)$ is the m.s. estimation error (variance) of $s(n)$ by $\hat{s}(n)$.

To start the filtering process we put:

$$\begin{aligned} \beta(1) &= \frac{\sigma_s^2}{\sigma_s^2 + \sigma_w^2(n)} \\ e(1) &= \frac{1}{\frac{1}{\sigma_s^2} + \frac{1}{\sigma_w^2(1)}} \\ \hat{s}(1) &= \beta(1)x(1) \end{aligned} \tag{39}$$

As it is possible to see the filter equations depend on ρ_1, the first correlation coefficient of the signal. Such a value can be regarded as a mere tuning parameter of the filter like v^2 in the Gaussian filter.

To make such an aspect of the filter clearer we have to determine the frequency response of the filter. Now $\alpha(n)$ and $\beta(n)$ depend only on ρ_1 and on the signal-to-noise ratio $r = \sigma_s^2/\sigma_w^2$. Thus to point out such a dependence we rewrite Eq. 31 as:

$$\hat{s}(n) - \beta(r, \rho_1)\hat{s}(n-1) = \alpha(r, \rho_1)x(n) \tag{40}$$

Now in z-transform notation (40) can be written as

$$(1 - \beta(r, \rho_1)z)\hat{s}(n) = \alpha(r, \rho_1)x(n) \tag{41}$$

From which we get the transfer function, $H(z)$:

$$H(z) = \frac{\alpha(r,\rho_1)}{1-\beta(r,\rho_1)z} \tag{45}$$

To obtain the frequency response, $u(f)$, where f indicates frequency or wavenumber indifferently, it suffices to compute (45) on the unit circle in the complex plane:

$$u(f) = \mid H(z) \mid^2 = \frac{\alpha(r,\rho_1)^2}{\mid (1-\beta(r,\rho_1)\exp(-2\pi i f \Delta x) \mid^2}; \quad z = \exp(-2\pi i f \Delta x) \tag{46}$$

where Δx denotes the sampling interval, in our context it is equivalent to the grid spacing. Also it must be noted that $f\Delta x$ is limited to Nyquist interval: $-1/2 \leq f\Delta x \leq 1/2$.

Now, once r is fixed, $u(f)$ depends only on ρ_1.

A 2-D Optimal Recursive Filtering Scheme

In this section it is illustrated how to use the filter equations above in order to perform a 2-D filtering.

Let us focus our attention on a HIRS scan line, say the i-th line. Let $X(i,j); \quad j = 1,\ldots,56$, denote the brightness temperature (or radiance) at the node (i,j). The line is filtered in the forward direction (from left to right) and at (i,j) node we get the improved estimate:

$$\hat{T}_F^R(i,j) = \beta_F^R(j)\hat{T}_F^R(i,j-1) + \alpha_F^R(j)X(i,j) \tag{47}$$

together with the error $\hat{\sigma}^2(\hat{T}_F^R(i,j))$, with the coefficients β and α and the error computed according to Eq.s (38). In (56) F and R indicate "forward" and "along the row" filtering respectively.

The same line is then filtered in the backward direction (from right to left) and at (i,j) node we obtain the estimate:

$$\hat{T}_B^R(i,j) = \beta_B^R(j)\hat{T}_B^R(i,j+1) + \alpha_B^R(j)X(i,j) \tag{48}$$

together with the error $\hat{\sigma}^2(\hat{T}_B^R(i,j))$, B denotes "backward" filtering.

Now we consider two lines above the i-th line an two line below and perform the recursive filtering along the columns. In the forward filtering (from above to below) we obtain at node (i,j):

$$\hat{T}_F^C(i,j) = \beta_F^C(i)\hat{T}_F^C(i-1,j) + \alpha_F^C(i)X(i,j) \tag{49}$$

together with the error $\hat{\sigma}^2(\hat{T}_F^C(i,j))$, C denotes filtering along the column.

In the backward filtering

$$\hat{T}_B^C(i,j) = \beta_B^C(i)\hat{T}_B^C(i+1,j) + \alpha_B^C(i)X(i,j) \tag{49}$$

together with the error $\hat{\sigma}^2(\hat{T}_B^C(i,j))$.

Finally, we combine the estimate aboves at (i,j) to give the final estimate $\hat{T}(i,j)$:

$$\begin{aligned}\hat{T}(i,j) = {} & \frac{\hat{T}_F^R(i,j)}{\hat{\sigma}^2(\hat{T}_F^R(i,j))} + \frac{\hat{T}_B^R(i,j)}{\hat{\sigma}^2(\hat{T}_B^R(i,j))} \\ & + \frac{\hat{T}_F^C(i,j)}{\hat{\sigma}^2(\hat{T}_F^C(i,j))} + \frac{\hat{T}_B^C(i,j)}{\hat{\sigma}^2(\hat{T}_B^C(i,j))}\end{aligned} \tag{50}$$

and its error:

$$\begin{aligned}\frac{1}{\hat{\sigma}^2(\hat{T}(i,j))} = {} & \frac{1}{\hat{\sigma}^2(\hat{T}_F^R(i,j))} + \frac{1}{\hat{\sigma}^2(\hat{T}_B^R(i,j))} \\ & + \frac{1}{\hat{\sigma}^2(\hat{T}_F^C(i,j))} + \frac{1}{\hat{\sigma}^2(\hat{T}_B^C(i,j))}\end{aligned} \tag{51}$$

Table captions

1 Values of d_m and d_r for five real cloudy conditions.

2 Summary of the results obtained by corrupting the test-field with real cloudy conditions.

OVERPASS	No. points	No. cloudy data	d_m	d_r
"1410"	4200	3690 (88%)	3.6	1.60
"1417"	4200	3648 (87%)	4.2	1.53
"1507"	4200	3334 (79%)	2.2	1.29
"1721"	4200	3626 (86%)	3.4	1.50
"1817"	4200	3774 (90%)	6.3	1.69

Tab. 1

	OVERPASS				
	"1410"	"1417"	"1507"	"1721"	"1817"
No. cloudy points	3690 (88%)	3648 (87%)	3334 (78%)	3626 (86%)	3774 (90%)
d_m	3.6	4.2	2.2	3.4	6.3
No. points restored:					
Gaussian scheme only	1193 (32%)	1020 (28%)	1798 (54%)	1102 (30%)	910 (24%)
Gaussian scheme + MSU regression relation	2497 (68%)	2628 (72%)	1536 (46%)	2524 (70%)	2864 (76%)
Mean Bias in the final field (°K):					
with de-biasing	0.08	0.07	0.04	0.04	0.06
without de-biasing	0.7	0.7	0.7	0.7	0.7
R.M.S. (°K):					
with de-biasing	0.25	0.32	0.20	0.25	0.33
without de-biasing	0.42	0.42	0.42	0.42	0.42

Figure captions

1 Arrangemrnt of HIRS radiances in grid. Δx correspond to the mean distance between two adjacent FOVs along a scan line in the HIRS scan pattern; Δy correspond to the line spacing.

2 Arrangement of HIRS data on circles for application in digital processing (objective Gaussian scheme).

Fig. 3 Adjacent HIRS FOVs used in the Gaussian filtering scheme with the central FOV.

Fig. 4 Pictorial represntation of a flag $CCF(i,j)$. There are 56 columns and 75 lines.

Fig. 5 Map of the zone of interest at which [redacted] data here analysed refer to.

Fig. 6 Flow-chart of the Gaussian filtering scheme.

Fig. 7 Mesh surface of the test-field. The test field consists of HIRS brightness temperature in channel 5 arranged in a grid 75x56.

Fig. 8 Test-field: plot of the line variances against the position of the line.

Fig. 9 Restoring the test-field after eliminating (randomly) 80% of data. The figure shows a mesh surface of the reconstructed field.

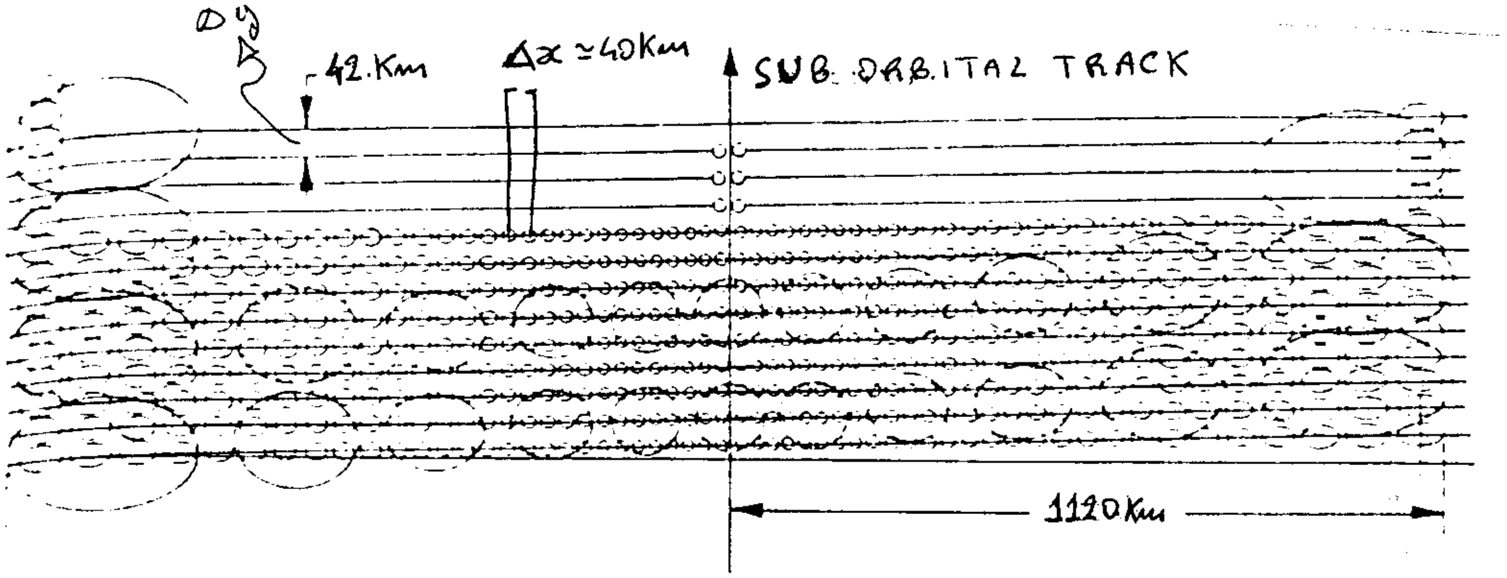
Δy
42 Km
Δx ≃ 40 Km
SUB ORBITAL TRACK
1120 Km

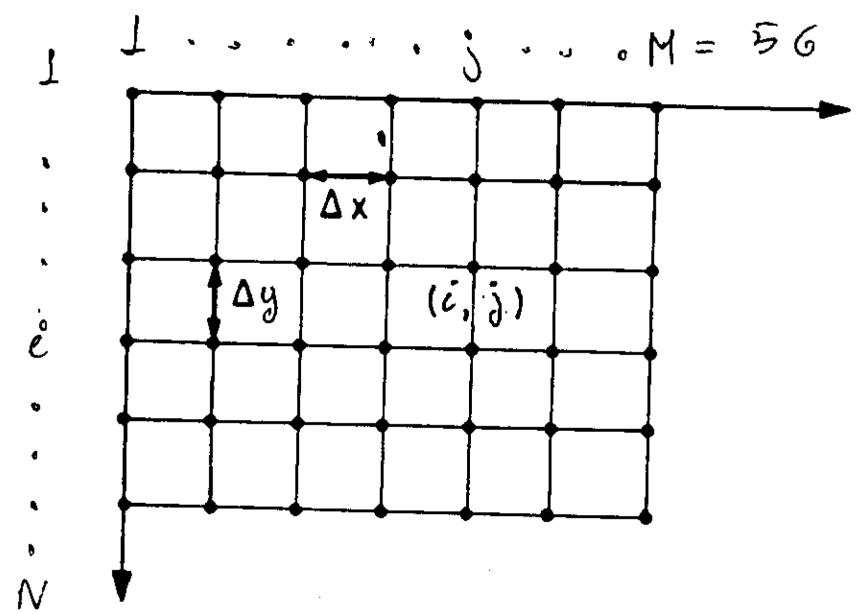
1 . . . . j . . . M = 56
1
i
N
Δx
Δy
(i, j)

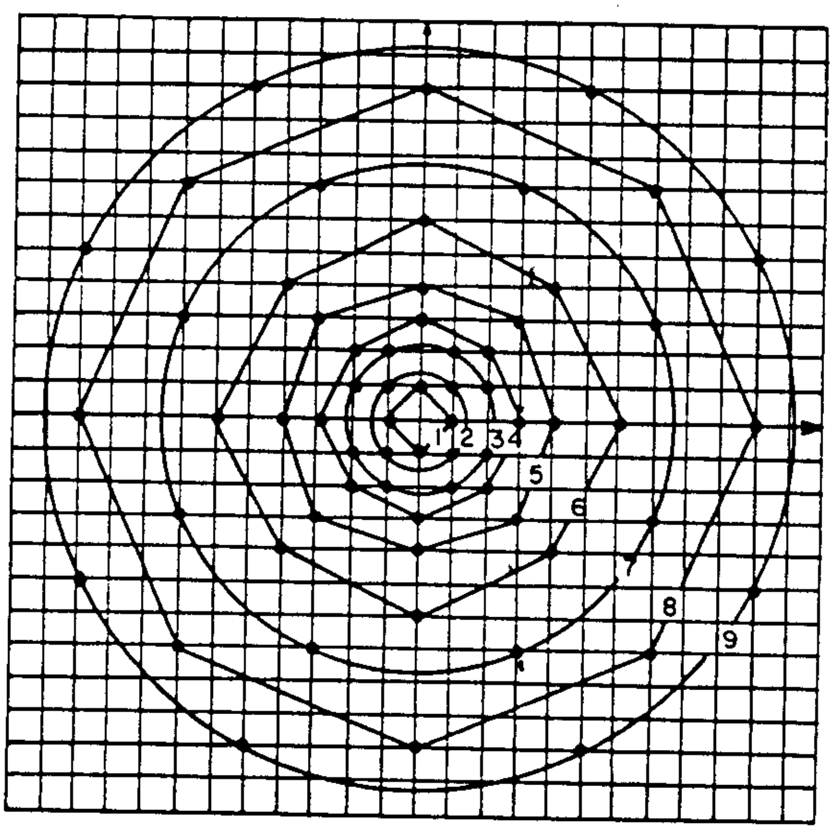

Circle Number	Average Radius
0	0
1	1
2	$\sqrt{2}$
3	$\sqrt{5}$
4	$\sqrt{8.5}$
5	$\sqrt{17}$
6	$\sqrt{34}$
7	$\sqrt{58}$
8	$\sqrt{99}$
9	$\sqrt{125}$

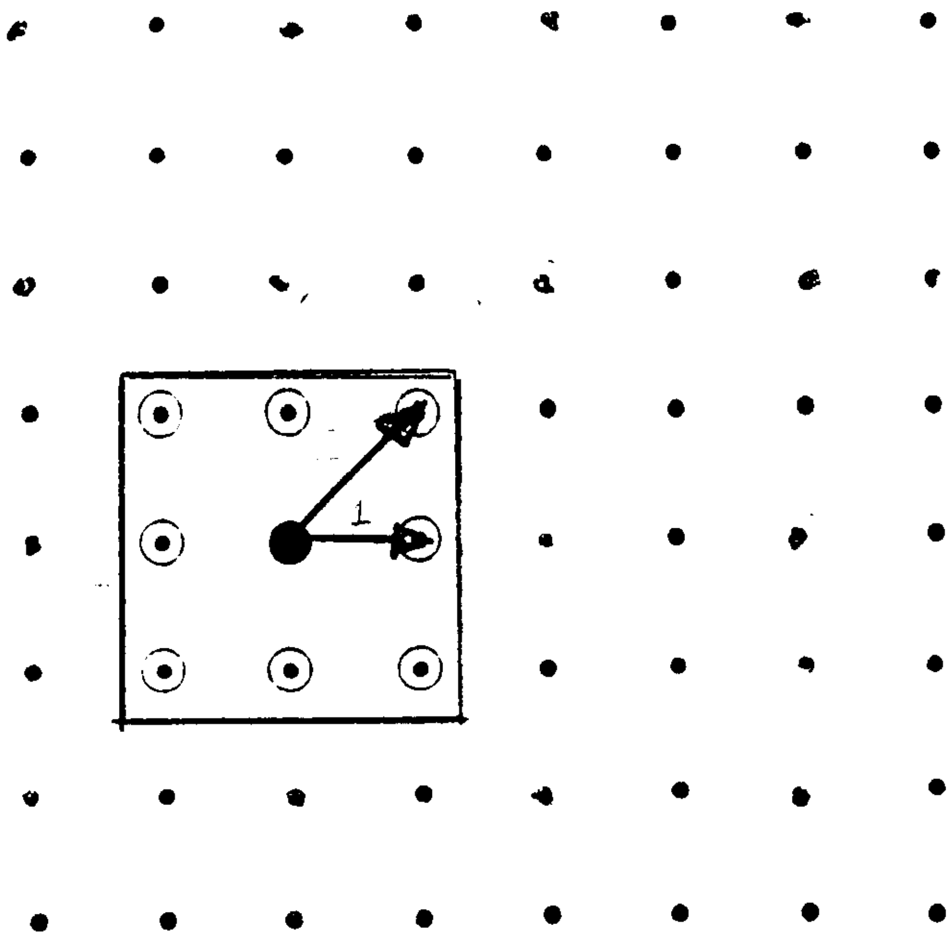
1

LINES

(75)

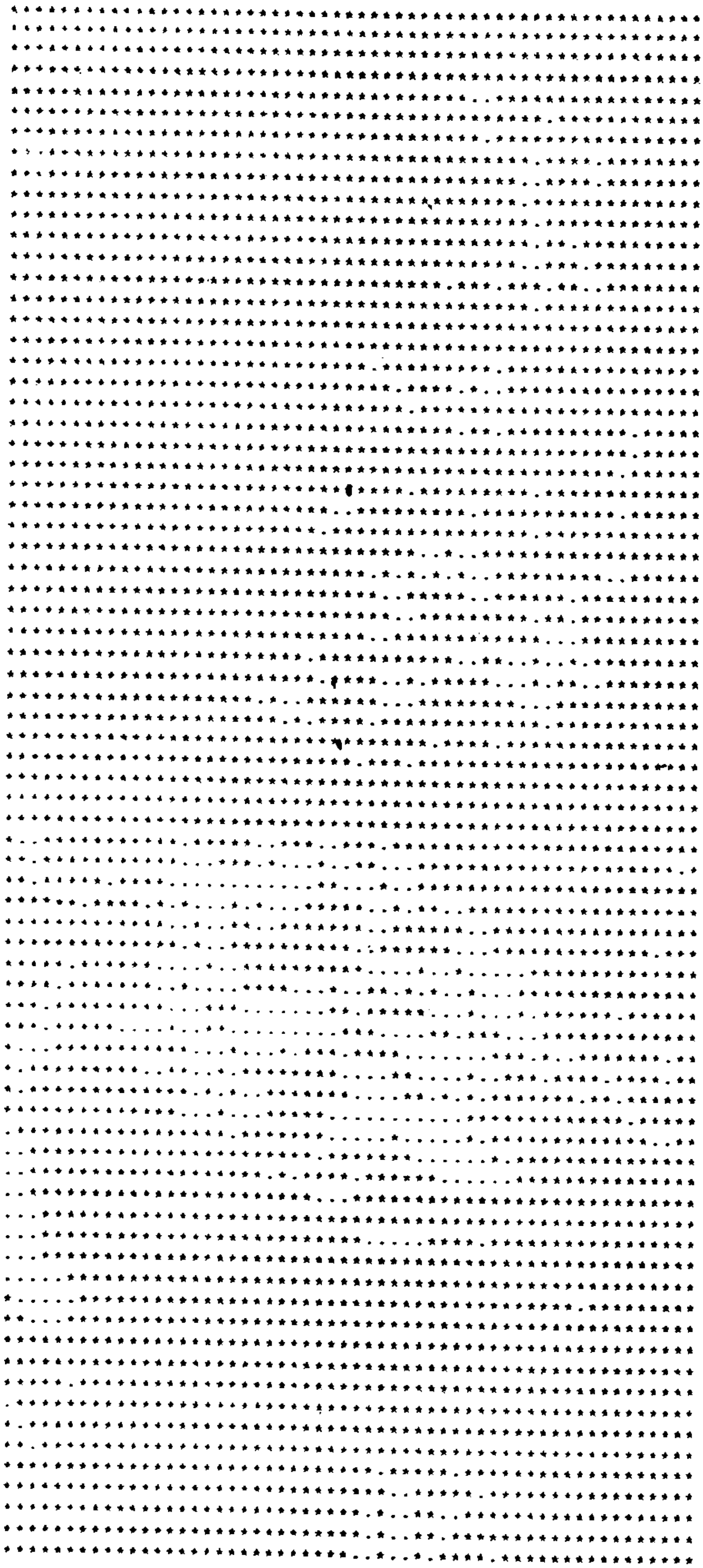

"." clear
"*" cloudy

"1807"

OVERPASS
on 14
DECEMBER, 1987

Fig. 4

Fig. 1

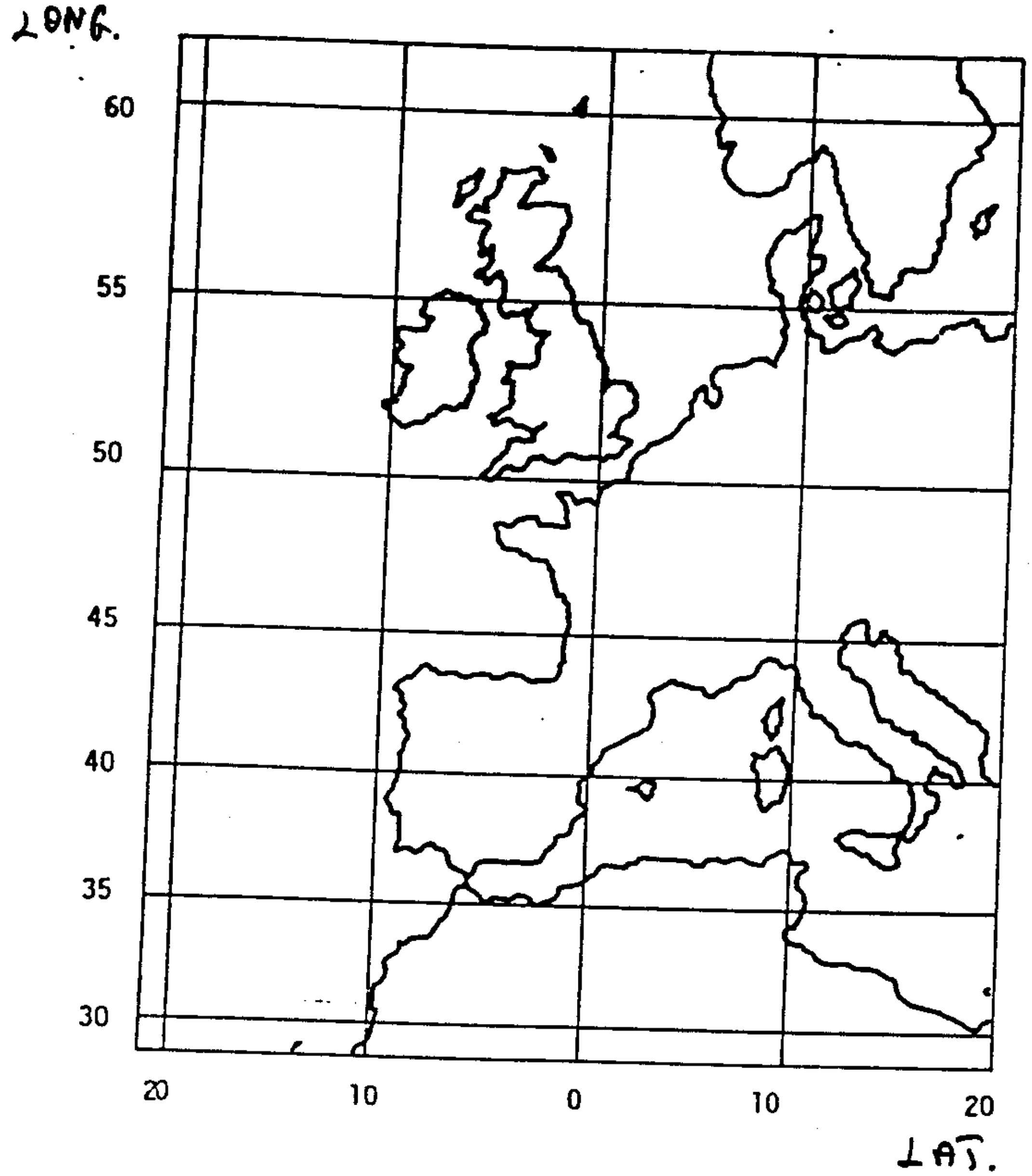

Fig. 5

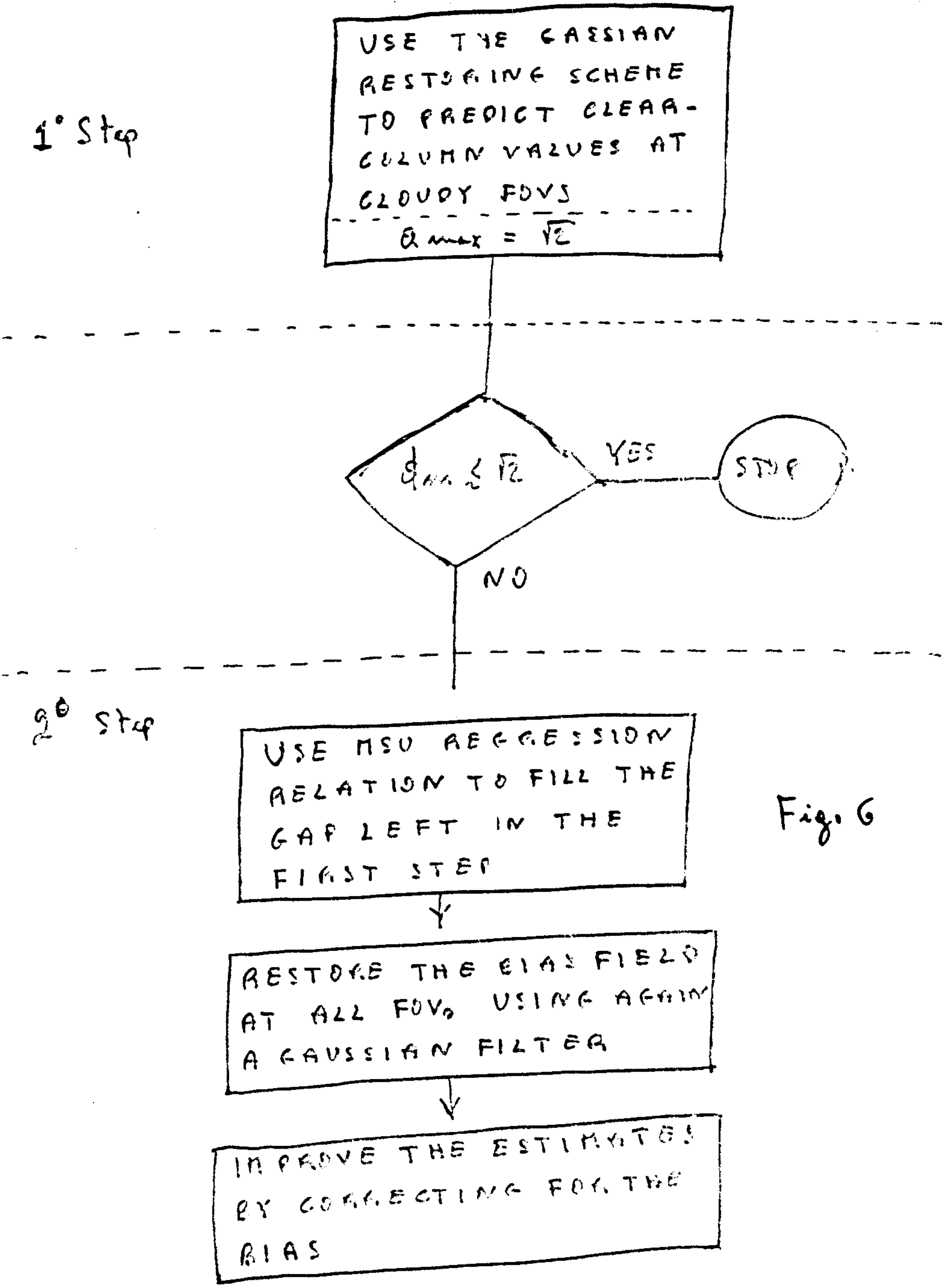

1° Step
USE THE GASSIAN RESTORING SCHEME TO PREDICT CLEAR-COLUMN VALUES AT CLOUDY FOVS
YES
STOP
NO
2° Step
USE MSU REGRESSION RELATION TO FILL THE GAP LEFT IN THE FIRST STEP
RESTORE THE BIAS FIELD AT ALL FOVs USING AGAIN A GAUSSIAN FILTER
IMPROVE THE ESTIMATES BY CORRECTING FOR THE BIAS

Fig. 6

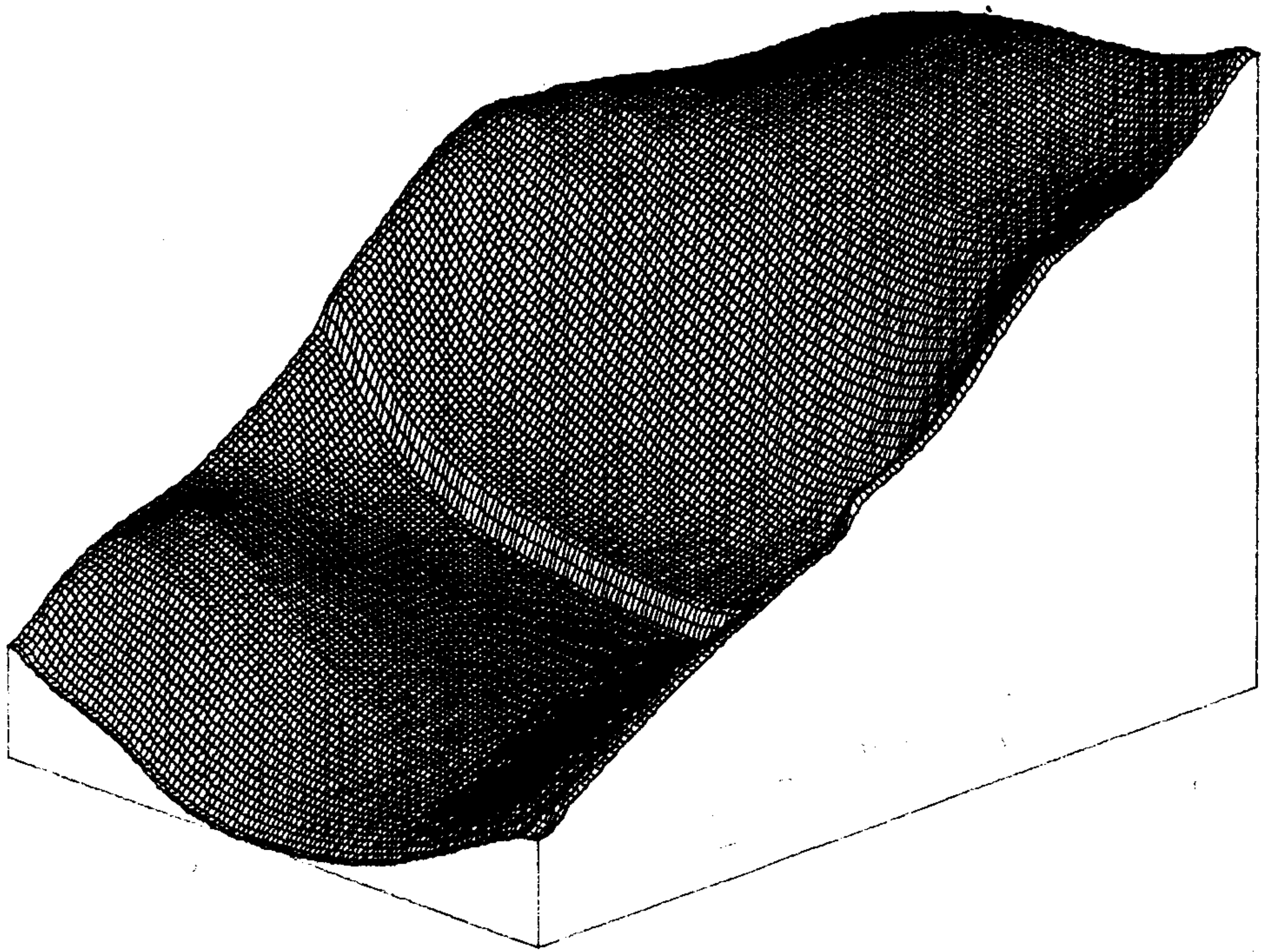
Fig 7

Fig. 8

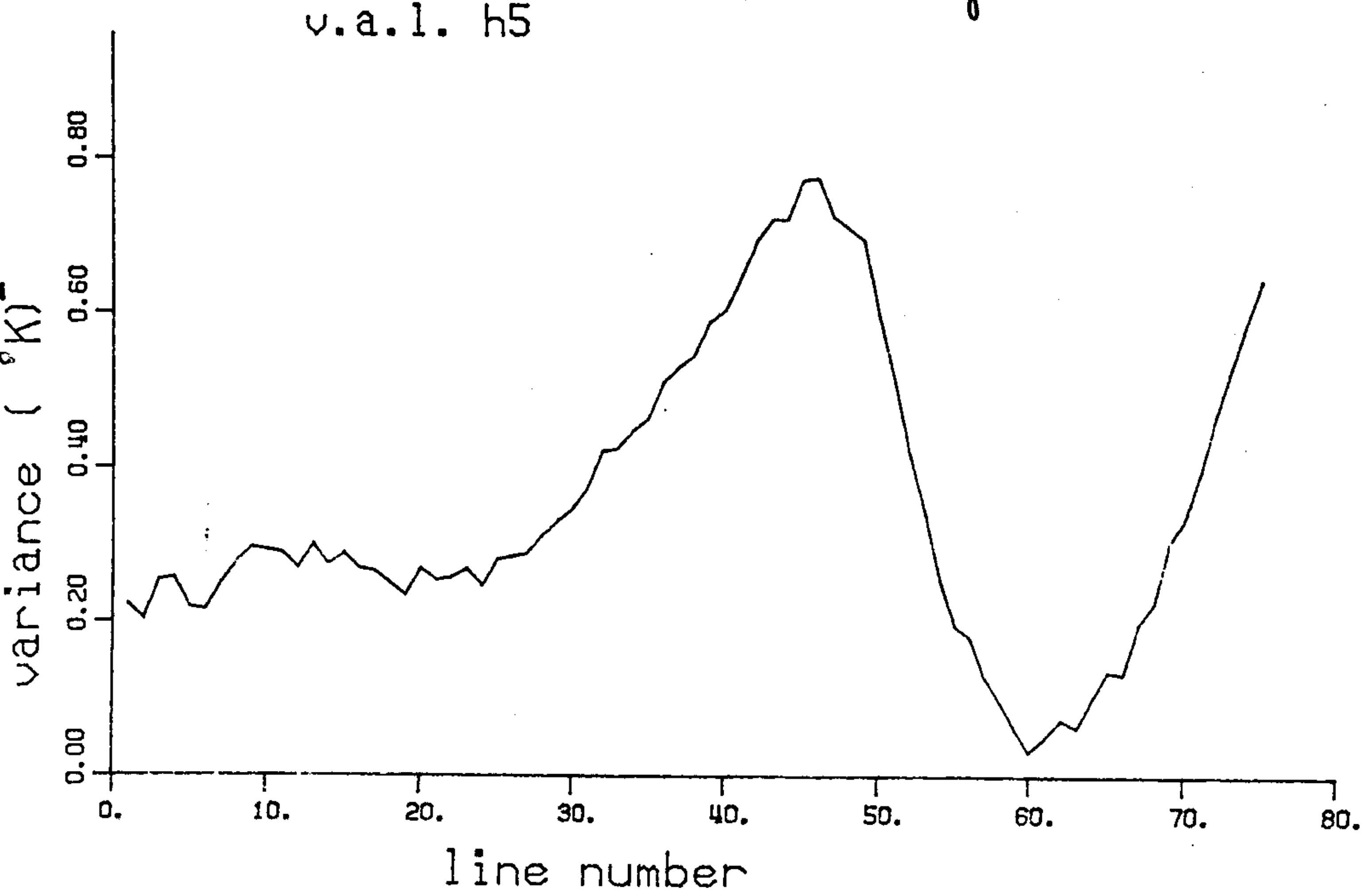

v.a.l. h5
variance (°K)²
0.00
0.20
0.40
0.60
0.80
0.
10.
20.
30.
40.
50.
60.
70.
80.
line number

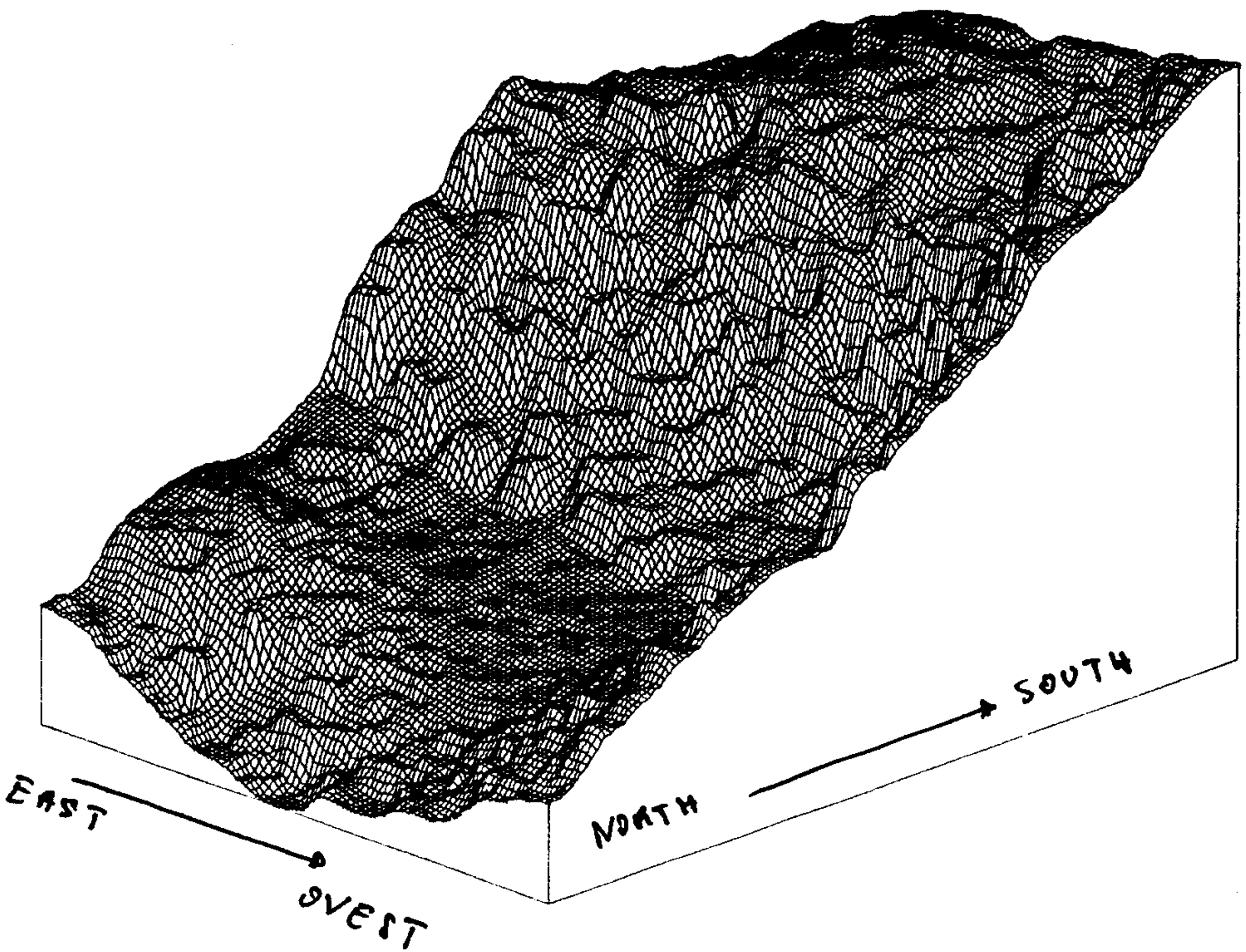

Fig. 9

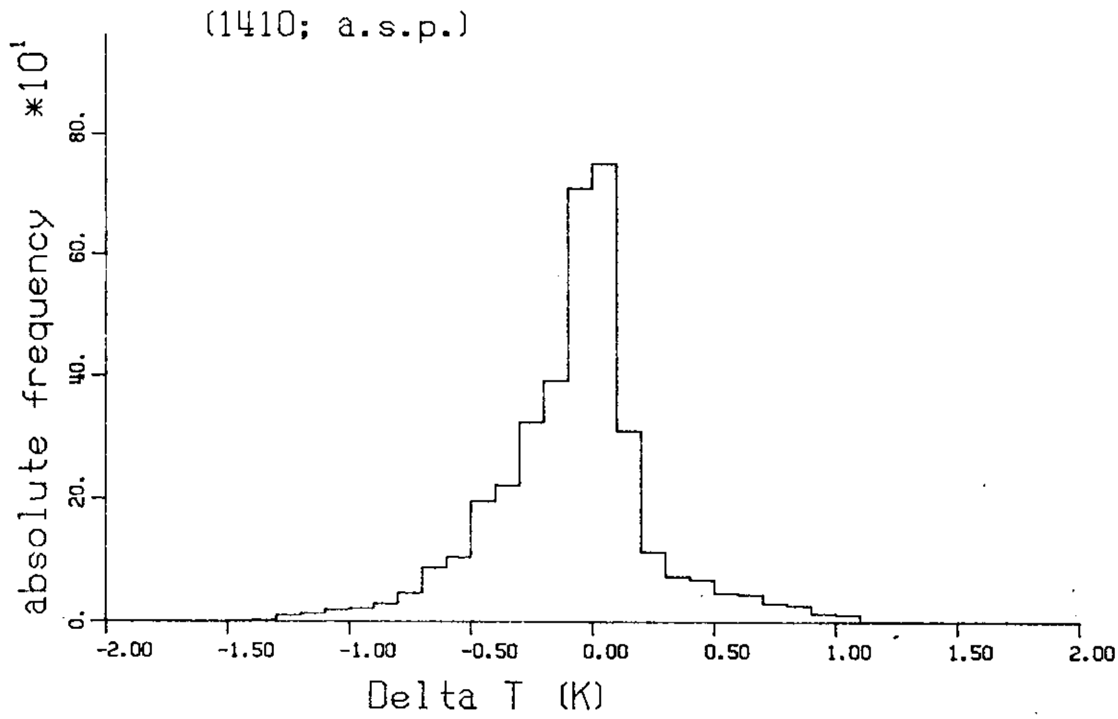

(1410; a.s.p.)
*10[1]
absolute frequency
0.
20.
40.
60.
80.
-2.00
-1.50
-1.00
-0.50
0.00
0.50
1.00
1.50
2.00
Delta T (K)

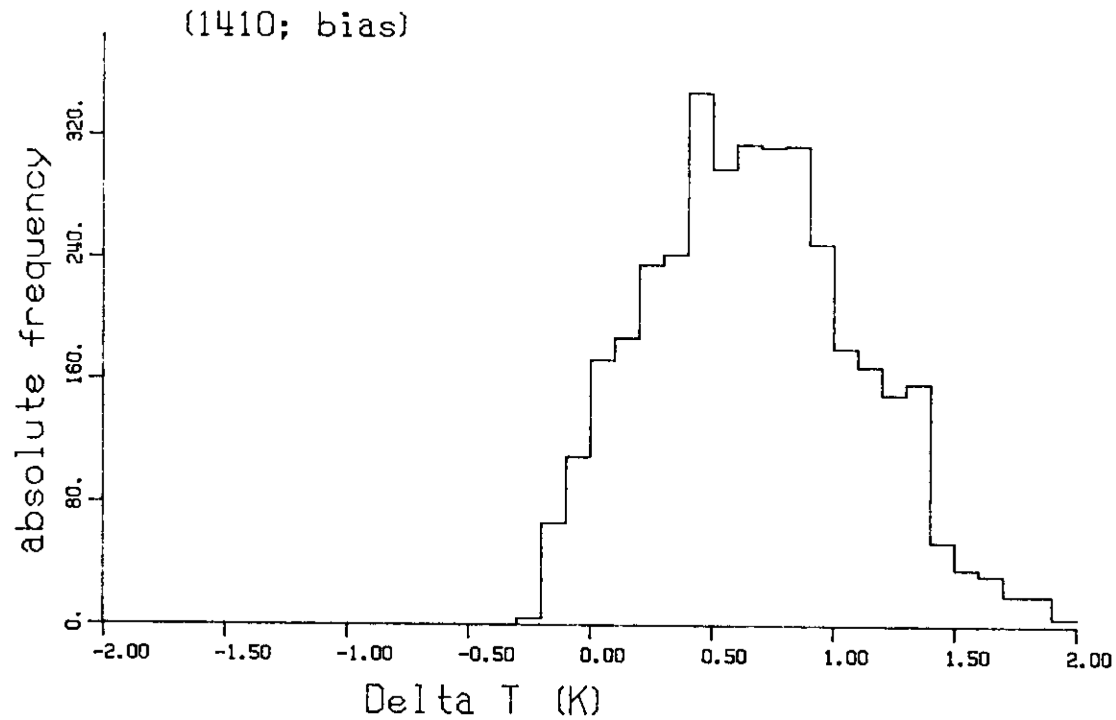

(1410; bias)
absolute frequency
0.
80.
160.
240.
320.
-2.00
-1.50
-1.00
-0.50
0.00
0.50
1.00
1.50
2.00
Delta T (K)

Fig. 10

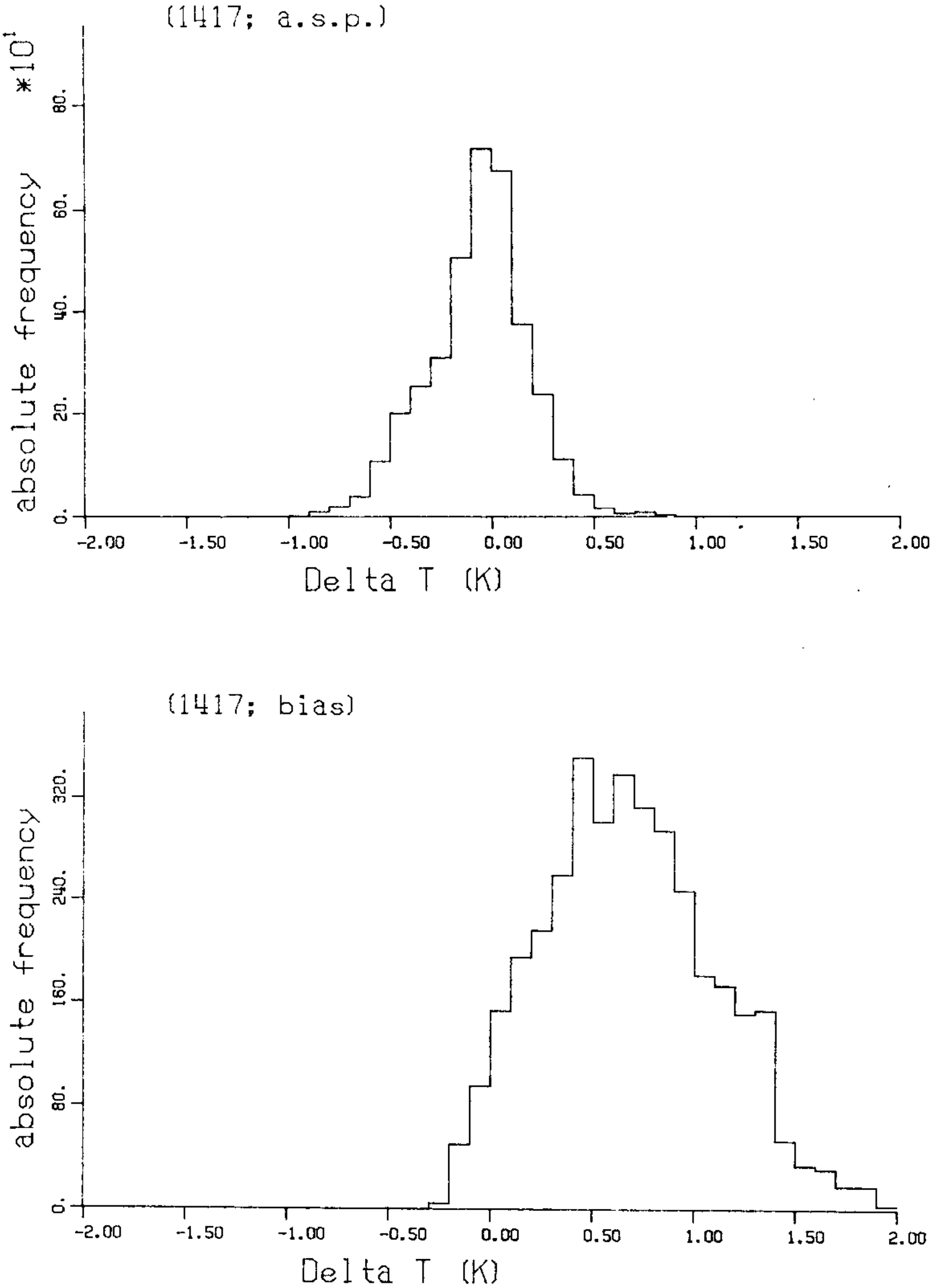

(1417; a.s.p.)
absolute frequency
*10¹
0.
20.
40.
60.
80.
-2.00
-1.50
-1.00
-0.50
0.00
0.50
1.00
1.50
2.00
Delta T (K)
(1417; bias)
absolute frequency
0.
80.
160.
240.
320.
-2.00
-1.50
-1.00
-0.50
0.00
0.50
1.00
1.50
2.00
Delta T (K)

Fig. 11

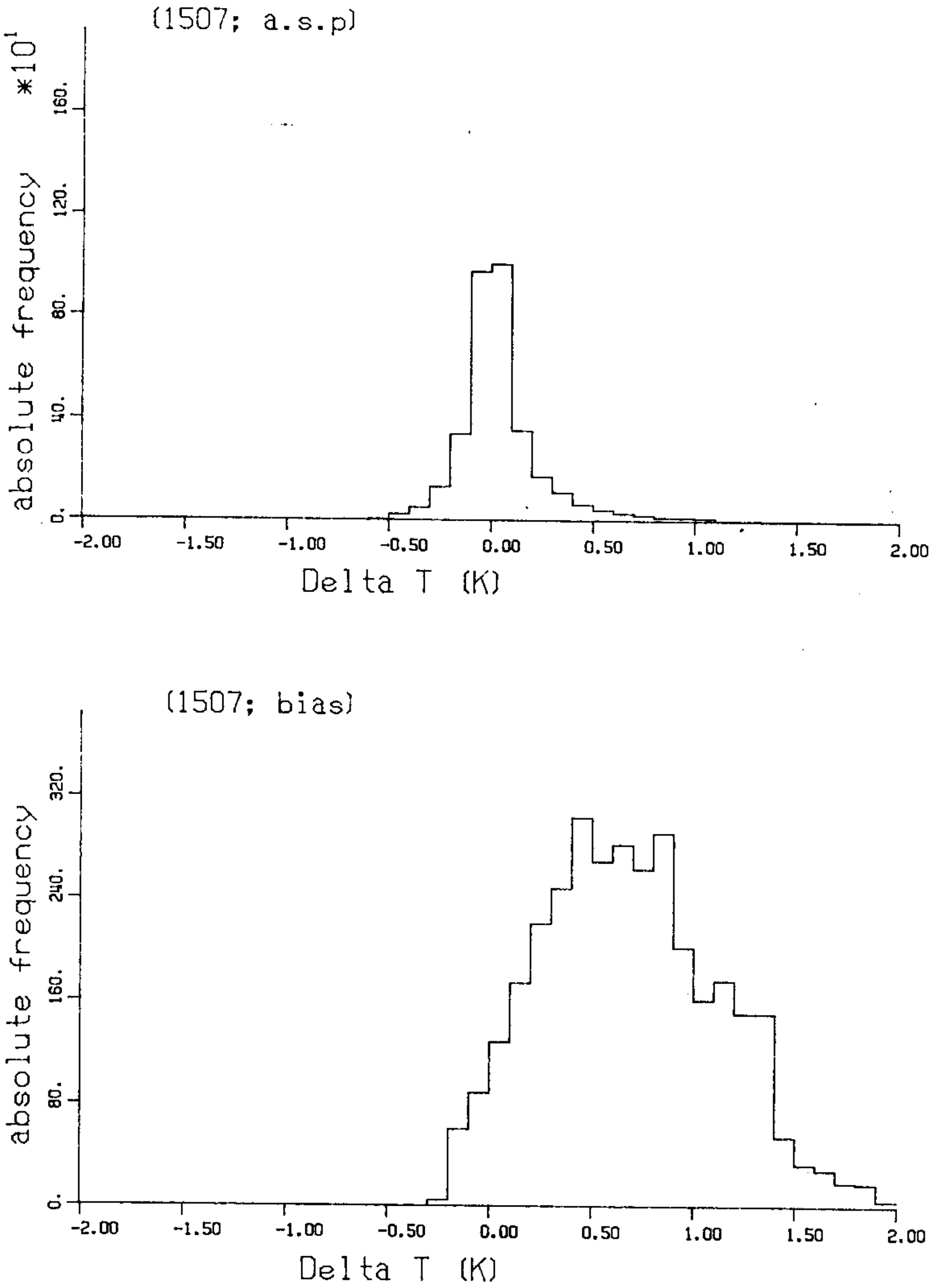
(1507; a.s.p)
*10[1]
absolute frequency
160.
120.
80.
40.
0.
-2.00
-1.50
-1.00
-0.50
0.00
0.50
1.00
1.50
2.00
Delta T (K)
(1507; bias)
absolute frequency
320.
240.
160.
80.
0.
-2.00
-1.50
-1.00
-0.50
0.00
0.50
1.00
1.50
2.00
Delta T (K)

Fig. 12

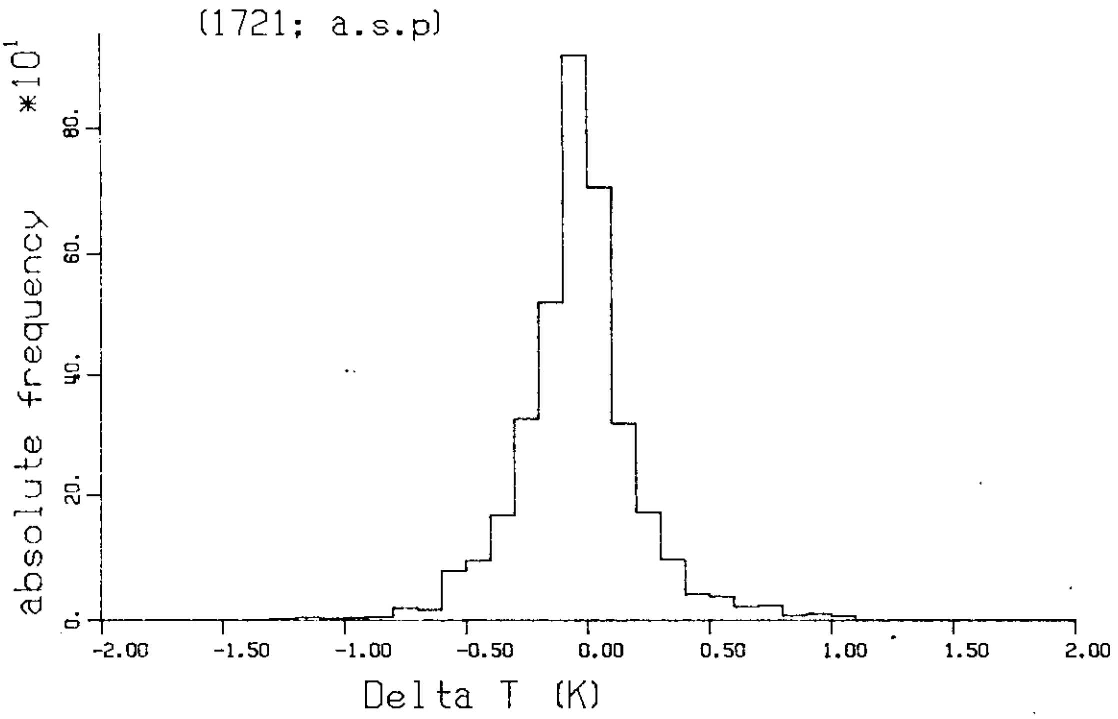
(1721; a.s.p)
absolute frequency *10[1]
0.
20.
40.
60.
80.
-2.00
-1.50
-1.00
-0.50
0.00
0.50
1.00
1.50
2.00
Delta T (K)

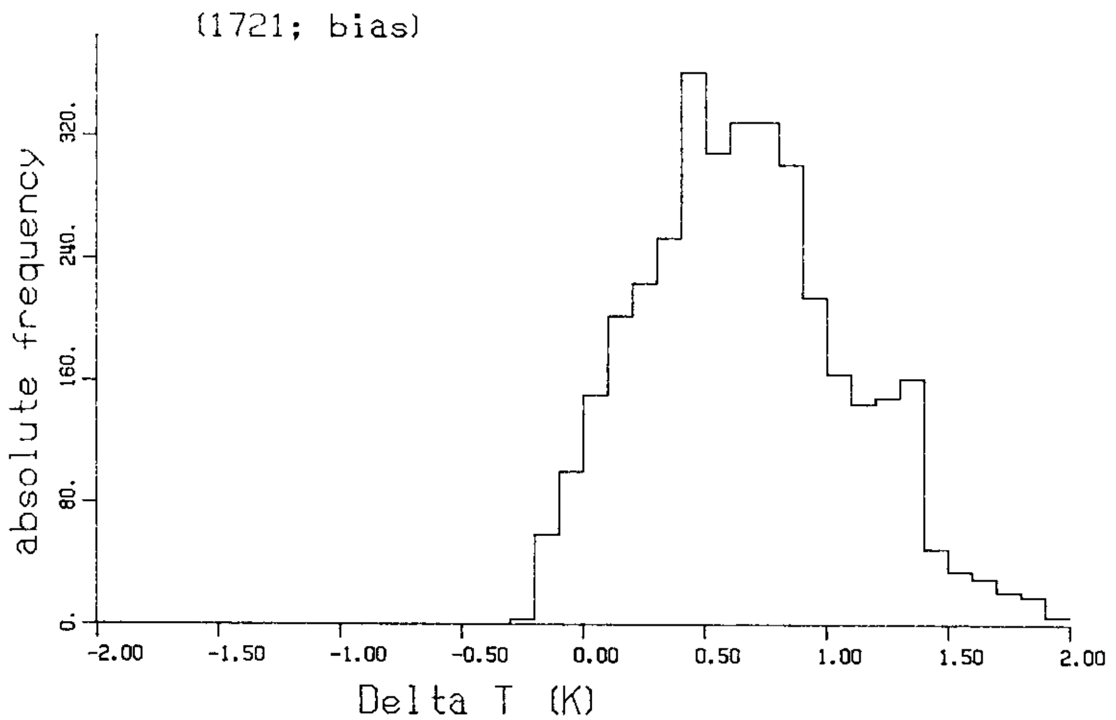
(1721; bias)
absolute frequency
0.
80.
160.
240.
320.
-2.00
-1.50
-1.00
-0.50
0.00
0.50
1.00
1.50
2.00
Delta T (K)

Fig. 13

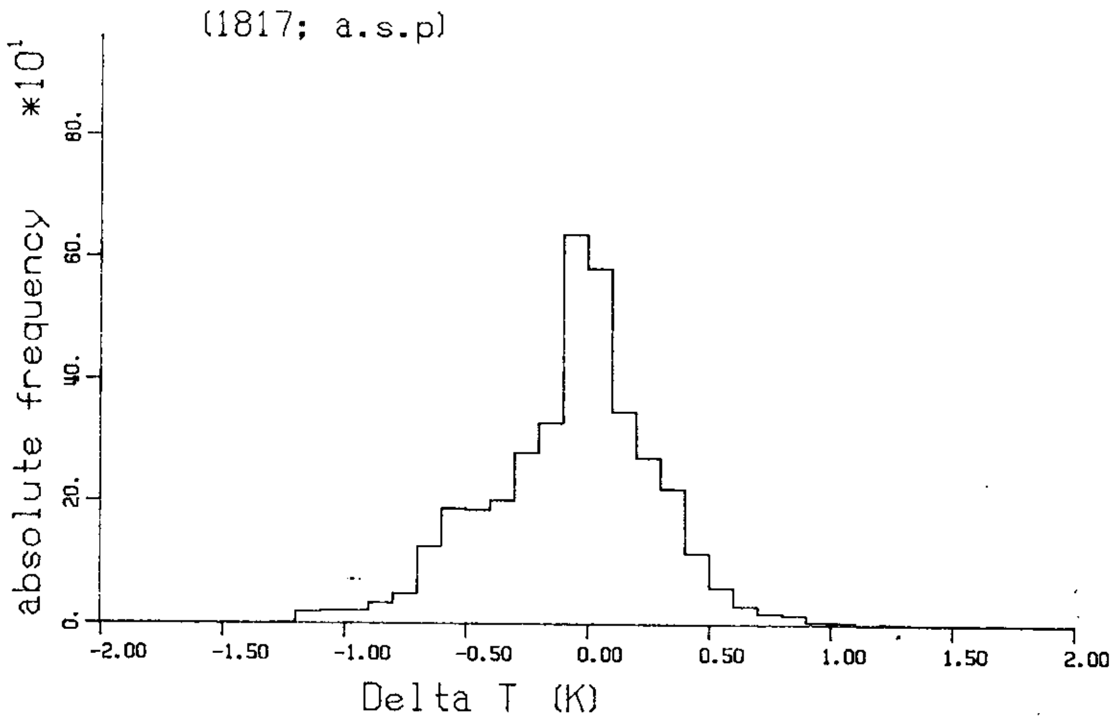

(1817; a.s.p)
*10¹
absolute frequency
0.
20.
40.
60.
80.
-2.00
-1.50
-1.00
-0.50
0.00
0.50
1.00
1.50
2.00
Delta T (K)

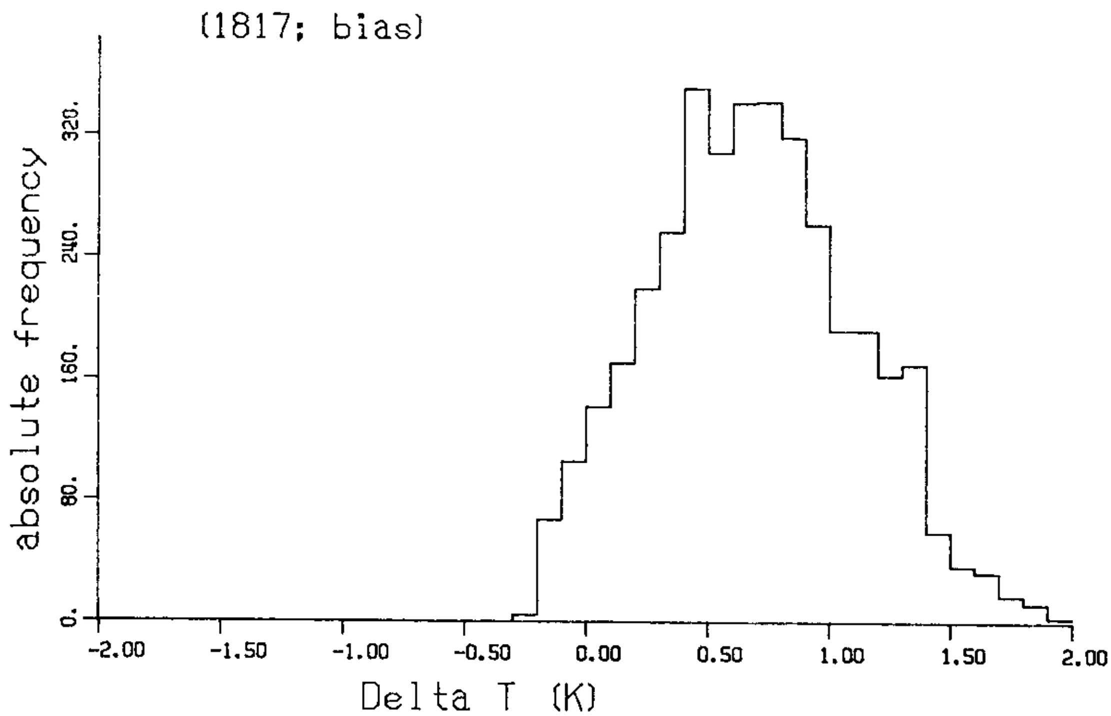

(1817; bias)
absolute frequency
0.
80.
160.
240.
320.
-2.00
-1.50
-1.00
-0.50
0.00
0.50
1.00
1.50
2.00
Delta T (K)

Fig. 14

References

1 Chedin A., and N.A. Scott (1984): Improved initialisation procedure ("3I"). Proceedings of the First International TOVS Study conference, Igls, Austria, CIMSS Report, Madison

2 Chedin A., N.A. Scott, C. Wahiche, P. Moulnier (1985): The omproved initialisation inversion method: A high resolution physical method for temperature retrievals for satellites of the TIROS-N series. JCAM, 24, 128-143

3 Eyre J. R. and P.D. Watts (1987): A sequential estimation approach to cloud-clearing for satellite temperature sounding. Q.J.R.Meteorol. Soc., 113, 1349-1376

4 Papoulis (1965): Probability, random variables and stochastic processes. McGraw Hill, New York

5 Robinson E. A. and M. T. Silvia (1981): Digital foundations of time series analysis. Wave-Equation, Space-Time Processing. Holden-Day, S. Francisco

6 [illegible]